

Received 24 March 2020; revised 25 May 2020; accepted 22 June 2020. Date of publication 24 June 2020; date of current version 15 July 2020.
The review of this article was arranged by Editor T.-L. Ren.

Digital Object Identifier 10.1109/JEDS.2020.3004618

MEMS-Based Planar Incandescent Microfilaments With Low Voltage Operation

JYUN-HAO LIAO¹, CHIEN-JU CHEN, CHIA-JUI YU¹, AND MENG-CHYI WU¹ (Senior Member, IEEE)

Institute of Electronics Engineering, National Tsing Hua University, Hsinchu 30013, Taiwan

CORRESPONDING AUTHOR: M.-C. WU (e-mail: mcwu@ee.nthu.edu.tw)

This work was supported by the Ministry of Science and Technology under Grant 107-2622-E-007-008-CC2 and Grant 108-2622-E-007-003-CC2.

ABSTRACT In this article, we report the design and fabrication for planar-type incandescent microfilaments on the silicon on insulator (SOI) wafer. The micro-electro-mechanical systems (MEMS) process with XeF₂ etching is used to construct the suspension structure for the reduction of thermal conduction. The fabricated line-type microfilament has a low operation voltage of 4 V. Besides, the operation voltages for the 1 × 4, 5 × 5, 6 × 6, and 7 × 7 arrays at 50 mtorr are 4.0, 9.0, 9.5, and 9.5 V, respectively. The 1 × 4 array filament exhibits the measured lifetime of 200 hrs and the predicted lifetime of about 570 hrs. The microfilament has a continuous broadband spectrum that covers from visible light extended to over 3 μm, which is a suitable light source for near-infrared spectroscopy.

INDEX TERMS Near-infrared spectroscopy, microfilament, array, MEMS, lifetime.

I. INTRODUCTION

Near-infrared (NIR) wavelength region is in the 900 to 2500 nm range which gets lots of attention in the applications of medical and physiological diagnostics, gas sensing, and food quality inspection. The main idea of NIR spectrometer is that illuminating the sample by NIR light source, functional groups in the sample such as C-H, O-H, and N-H would absorb the specific wavelengths of incident light. Thus, the obtained sample's absorption spectra vary with the type and concentration of the functional groups and present the significant differences. Therefore, the data can be analyzed to show the agricultural products' compositions like water, sugar, protein, fiber, fat, and starch [1]–[3].

Light emitting diode (LED) and semiconductor laser are commonly used semiconductor light sources nowadays for many advantages owing to their well-developed techniques. However, it is difficult to have a continuous broadband output spectrum for LEDs. Although halogen lamp has a broadband emission spectrum, large volume and power consumption usually limit its applications. It is necessary to develop the microfilament that incandesces as a light source with emitting the broadband spectrum for near-infrared

spectroscopy (NIRS) [4]–[6]. Incandescence is the emission which radiates from a thermal object and is known as the blackbody radiation [7]. The mechanism of incandescent filament is electrical resistive heating, which converts the input electrical power to heat [8]. The critical design is the thermal isolation structure to sustain the operation temperature of the filament [9].

Previous reports show the filament light sources with kinds of materials, however, operation voltages were too high to be used for the portable devices. Tu *et al.* reported the silicon filament coated with silicon nitride has an operation voltage of about 8 V with continuous operation for 10 hrs for the spectrophotometric microsystem [5]. Tuma *et al.* demonstrated the fabricated tungsten spiral filaments had an operation voltage of 7.36 V at the driving current of 170 mA [4]. Alayo *et al.* reported the microlamp, which filament was made of chromium film, can be operated at 20 V and 35 mA [10].

In this article, we report the design and fabrication of the low-voltage operated filament, which is the lowest to the prior arts, in line shape and planar type on the silicon on insulator (SOI) wafers by using micro-electro-mechanical

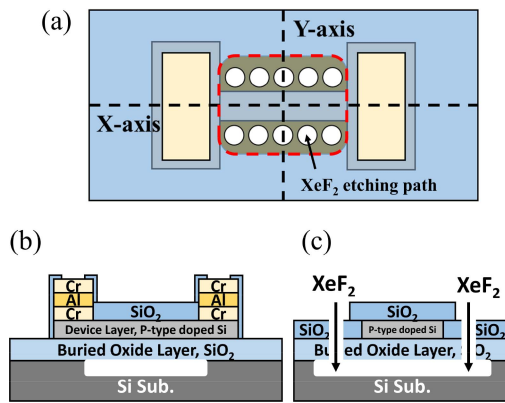


FIGURE 1. Schematics of suspension structure of microfilament after dry etching process: (a) top view of the device, (b) and (c) cross section views along X- and Y-axes accordingly which indicated in the top view. The red dash line in top view shows the area which Si substrate is etched by XeF₂ to reduce the thermal conduction path of substrate.

systems (MEMS) process [10]–[12]. The suspension structure is fabricated simpler by introducing XeF₂ isotropic etching, which can effectively suppress the heat conduction by highly selective etch for Si substrate. Also, the microfilament arrays are further fabricated to exhibit the low operation voltages of 4.0, 9.0, 9.5, and 9.5 V for the array formats of 1 × 4, 5 × 5, 6 × 6, and 7 × 7, respectively. In addition, the filaments also show a broadband emission spectrum and the expected long lifetime of over 570 hrs.

II. EXPERIMENTAL

Three types of SOI wafers are used for the microfilament fabrication. All the SOI wafers have a buried oxide thickness of 1 μm, which is served as either electrical or thermal isolation of microfilament while in operation. Wafers SOI-A, SOI-B, and SOI-C have the boron-doped p-type device layer thickness of 3 ± 0.5, 5 ± 0.5, and 2 ± 0.5 μm, which correspond to the resistivity of 0.01–0.1, 0.001–0.005, and 0.001–0.005 ohm-cm, respectively. The specification shows that the resistivity of SOI-B and SOI-C are the same, however, measured by Hall method, the doping concentration of Wafer SOI-C is $9.4 \times 10^{19} \text{ cm}^{-3}$ which is higher than that of $5.3 \times 10^{19} \text{ cm}^{-3}$ of Wafer SOI-B. The suspension structure is implied to isolate the microfilament thermally from the substrate, permitting the microfilament to maintain enough heat and emit the light. The etching gas XeF₂ is used in MEMS fabrication process widely for its highly selective characteristic for Si etching from other materials. Besides, it is easy to make the etching mask by SiO₂ or photoresist.

Fig. 1(a) shows the top view of the device and Fig. 1(b) and 1(c) show the schematic cross section views along X- and Y-axes of line-type microfilament for better understanding of the suspension structure. The designed suspension structure let filament be encompassed by air which has low thermal conductivity. The incandescent area of microfilament is first defined by dry etching on the high doping Si

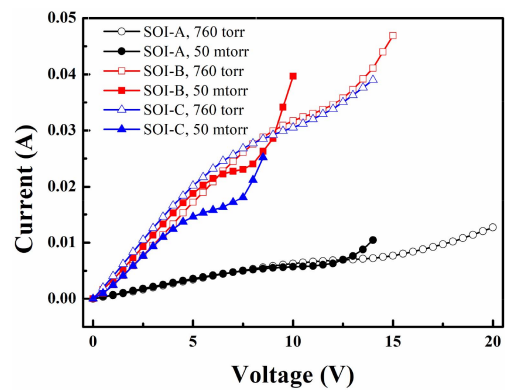


FIGURE 2. Current versus voltage (I-V) characteristics measured at 760 torr and 50 mtorr of line-type microfilaments with a length of 1330 μm and a width of 90 μm fabricated from Wafers SOI-A, SOI-B, and SOI-C.

device layer. The contact metal pad composed of Cr/Al/Cr (30 nm/400 nm/30 nm) is then deposited by thermal coater. The bottom metal Cr is used as an adhesion layer and the top metal Cr is used to avoid the oxidation of Al. The thick Al layer is mainly for better contact when probing. Afterward, the SiO₂ passivation layer is deposited by plasma-enhanced chemical vapor deposition (PECVD) to make both thermal and electric isolations of microfilament. The XeF₂ etching paths around the microfilament are defined by reactive ion etching (RIE) through the SiO₂ passivation layer to the buried oxide layer and the Si substrate. Finally, the suspension structure is formed without damaging the device layer of SOI wafer.

The microfilament is placed on a copper seat in the vacuum probe system and the source meter Tektronix 2410 is used to supply the steady direct current. The chamber in a vacuum environment was kept at about 50 mtorr. The light emitted from the operating component was received by the optical fiber and the spectrometer for the analyses of both electrical and optical characteristics.

III. RESULTS AND DISCUSSION

Fig. 2 shows the current as a function of biased voltage (I-V) measured at 760 torr and 50 mtorr for the microfilaments fabricated from Wafers SOI-A, SOI-B, and SOI-C. All the microfilaments have a line shape with a length of 1330 μm and a width of 90 μm. In the I-V curves, the turn point that device current increase rapidly is defined as operation voltage, which can be seen more clearly at lower pressure. The current initially increases with biased voltage for all the filaments. However, at 50 mtorr, the current rapidly increases at 8 and 7.5 V for the devices fabricated from Wafers SOI-B and SOI-C, respectively, and at 12 V for the device fabricated from Wafer SOI-A. Above the turn point voltage, the current will be incandescent. On the other hand, the filament fabricated from Wafer SOI-A has the highest resistance while the other two fabricated from Wafers SOI-B and SOI-C have almost the same low resistance, just as mentioned in the Experimental. For the low-resistivity filament

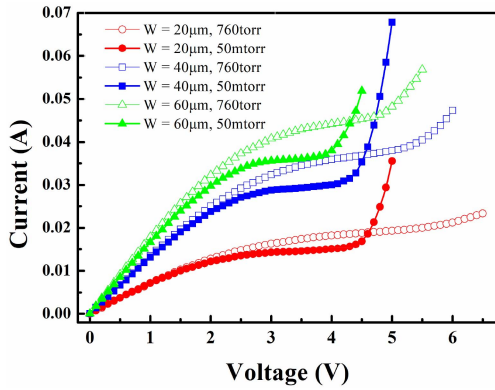


FIGURE 3. Current-voltage characteristics measured at 760 torr and 50 mtorr of line-type microfilaments with the same length of 400 μm and the widths of 20, 40, and 60 μm fabricated from Wafer SOI-C.

at the same bias voltage, there is a higher current density passing through the filaments. It would make the devices fabricated from Wafers SOI-B and SOI-C easily gather sufficient amount of heat and incandesce the filaments. It means that the devices fabricated from Wafers SOI-B and SOI-C have a lower operation voltage. Although Wafers SOI-B and SOI-C have the same resistivity, Wafer SOI-C with a higher doping concentration and a thinner device layer is the best choice to reduce the operation voltage. Therefore, the filaments in the further studies were fabricated from Wafer SOI-C. In order to reduce the operation voltage, the fabricated filaments are scaled down proportionally to keep the same resistance, while the incandescent area is the only difference which results in different heat dissipation areas. Larger heat dissipation area means it is more difficult to preserve the heat; therefore, the device needs a higher operation voltage to gain more thermal energy that acquires to incandesce.

Fig. 3 shows the I-V characteristics of line-type microfilaments with the same length of 400 μm and the widths of 20, 40, and 60 μm . To verify the effects of air convection on operation voltage, devices were measured at 50 mtorr and 1 atm. The filaments have a higher operation voltage to incandesce at 760 torr than those at 50 mtorr. Meanwhile, the filament with a wider width has a lower operation voltage to incandesce. The operation voltages at 760 torr are about 5.7, 5.3, and 4.8 V for the filaments with the widths of 20, 40, and 60 μm , respectively. On the other hand, the operation voltages at 50 mtorr are about 4.5, 4.3, and 4 V for the filaments with the widths of 20, 40, and 60 μm , respectively. The lowest operation voltage can be obtained to be 4.0 V at 50 mtorr and 4.8 V under atmosphere for the filament with 60 μm in width. The corresponding passing currents are 37.0 and 48.2 mA, respectively. The low operation voltage of filament is attributed to the low resistance and thus the wider filament width.

The emission spectra of the filament with a length of 400 μm and the width of 60 μm biased at 4.0, 4.5, and 5.0 V are showed in Fig. 4. An increase of the biased voltage leads

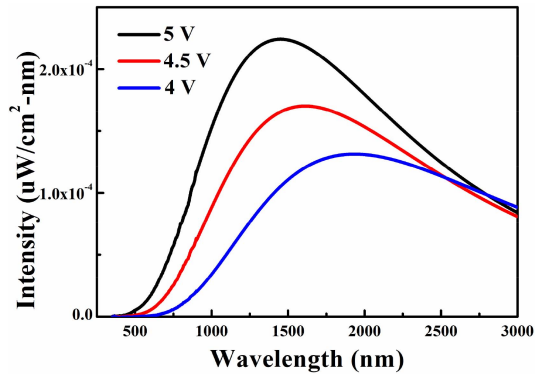


FIGURE 4. The emission spectra of the filament with a length of 400 μm and the width of 60 μm biased at 4.0, 4.5, and 5.0 V.

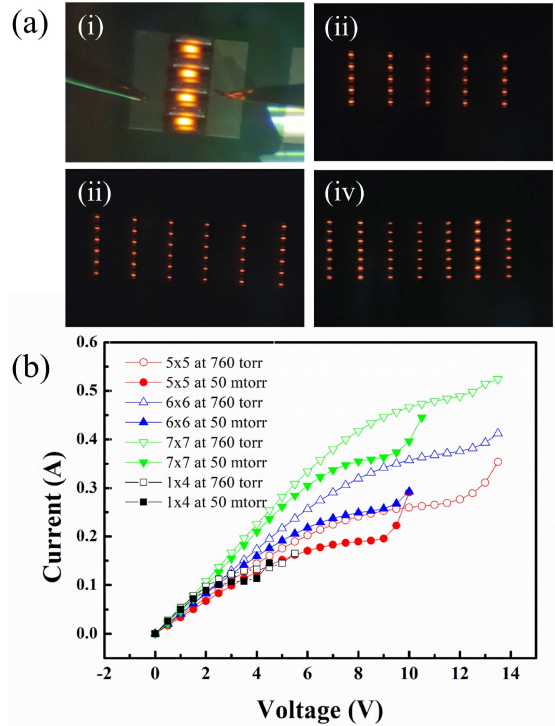


FIGURE 5. (a) Photographs of microfilament arrays of (i) 1 \times 4, (ii) 5 \times 5, (iii) 6 \times 6 and (iv) 7 \times 7 under incandescent condition. Each line of microfilament has a size of 400 μm in length and 60 μm in width and is connected in parallel. (b) Current-voltage characteristics of each array measured at 760 torr and 50 mtorr.

to the increase of the peak intensity of spectrum. The peak intensity is $1.3 \times 10^{-4} \mu\text{W}/\text{cm}^2\text{-nm}$ at 4.0 V. Meanwhile, the filament exhibits the peak wavelength of 1450, 1615, and 1935 nm at 4.0, 4.5, and 5.0 V, respectively. The emission spectra can extend to over 3 μm which shows great potential in the applications of NIRS.

Fig. 5(a) shows the photographs of line-type microfilament array of (i) 1 \times 4, (ii) 5 \times 5, (iii) 6 \times 6, and (iv) 7 \times 7 under incandescent condition. Each line of microfilament has a size of 400 μm in length and 60 μm in width and is connected in parallel. The applied voltage is biased on the two ends of metal pads which are not on the suspension structure.

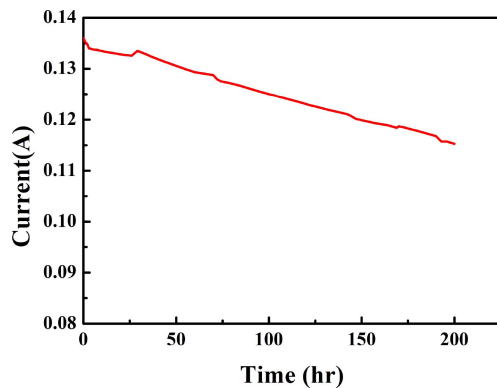


FIGURE 6. Lifetime measurement of line-type 1×4 microfilament array with a length of $400 \mu\text{m}$ and the width of $60 \mu\text{m}$ for 200 hrs under the constant bias of 4.75 V and continuous operation.

Fig. 5(b) shows the I-V characteristics of 1×4 , 5×5 , 6×6 , and 7×7 arrays of line-type microfilament measured at the pressures of 760 torr and 50 mtorr. As described earlier, the turn point voltage of the microfilament arrays occurs at a lower voltage at 50 mtorr than that at 760 torr. The turn point voltages and currents for the 1×4 , 5×5 , 6×6 , and 7×7 arrays at 50 mtorr are 4.0, 9.0, 9.5, and 9.5 V and 113.9, 195.4, 267.4, and 373.5 mA, while those at 760 torr are 5.0, 12.5, 13.0, and 13.0 V and 144.6, 289.4, 393.3, and 514.3 mA, respectively. An increase of array number would increase the device resistance and thus the turn point voltage to incandescence the filaments. The 1×4 array shows a much smaller turn point voltage than other large format arrays because the larger arrays have the higher resistance contributed by the longer electrical path from the electrode pads. Based on the parallel connection of microfilaments in the array, each array has the same turn point voltage, however, the larger array, which has a longer electrical path, would result in higher resistance. Thus the microfilament array with larger number has a higher turn point voltage.

The lifetime of microfilament is also an important issue for a light source. Fig. 6 shows the current-versus-time plot under the constant bias of 4.75 V for the 1×4 filament with a length of $400 \mu\text{m}$ and the width of $60 \mu\text{m}$. The line-type microfilament can be lightened on up to 200 hrs under continuous operation. The decay tendency is close to the gradually decay model and is adequate to use linear fit for lifetime prediction. The decrease of current is caused by the increase of resistance due to the nonuniform defects generated on the device layer after long-time incandescence

of microfilament. Setting 70% of initial current value as a lifetime reference point, the estimated lifetime is beyond 570 hrs by linear fit to the current-versus-time plot.

IV. CONCLUSION

The MEMS-based line-type microfilaments with XeF_2 dry etching process are successfully applied to construct the suspension structure which effectively reduces the heat dissipation and lowers the operation voltage. The fabricated microfilament exhibits an operation voltage of 4 V and the 1×4 array filament has the measured lifetime of 200 hrs and the predicted lifetime of about 570 hrs. The microfilament has a continuous broadband output spectrum that covers from visible light extended to over $3 \mu\text{m}$, which is a suitable light source for NIRS.

REFERENCES

- [1] K. B. Walsh, M. Golic, and C. V. Greensill, "Sorting of fruit using near infrared spectroscopy: Application to a range of fruit and vegetables for soluble solids and dry matter content," *J. Near Infrared Spectrosc.*, vol. 12, pp. 141–148, Sep. 2004.
- [2] H. Maeda and Y. Ozaki, "Near infrared spectroscopy and chemometrics studies of temperature-dependent spectral variations of water: Relationship between spectral changes and hydrogen bonds," *J. Near Infrared Spectrosc.*, vol. 3, pp. 191–201, Aug. 1997.
- [3] F. F. Jöbsis, "Noninvasive, infrared monitoring of cerebral and myocardial oxygen sufficiency and circulatory parameters," *Science*, vol. 198, pp. 1264–1267, Dec. 1977.
- [4] M. L. Tuma, K. King, H. L. Kim, R. Hansler, E. W. Jones, and T. George, "MEMS incandescent light source," in *Proc. SPIE Photon. Space Environ. VII*, vol. 4134, Oct. 2000, pp. 151–158.
- [5] J. Tu, D. Howard, S. D. Collins, and R. L. Smith, "Micromachined, silicon filament light source for spectrophotometric microsystems," *Appl. Opt.*, vol. 42, no. 13, pp. 2388–2397, 2003.
- [6] A. H. Gollub, D. O. Carvalho, G. Rehder, and M. I. Alayo, "Development of micro-incandescent light sources on silicon substrate," *Proc. SPIE Micromach. Microfab. Process Technol. XV*, vol. 7590, 2010, pp. 75900E1–75900E10.
- [7] W. E. Forsythe and E. Q. Adams, "Radiating characteristics of tungsten and tungsten lamps," *J. Opt. Soc. America*, vol. 35, pp. 108–113, Feb. 1945.
- [8] D. Maclsaac, G. Kanner, and G. Anderson, "Basic physics of the incandescent lamp," *Phys. Teach.*, vol. 37, pp. 520–525, Dec. 1999.
- [9] D. O. Carvalho, M. N. P. Carreño, G. P. Rehder, and M. I. Alayo, "Integrated incandescent microlamp coupled to SiO_xN_y waveguide," in *Proc. SPIE MOEMS Miniaturized Syst. VIII*, vol. 7208, Feb. 2009, pp. 72080U-1–72080U-10.
- [10] M. Alayo, G. Rehder, and M. N. P. Carreño, "MEMS-based incandescent microlamps for integrated optics applications," *J. Opt. A, Pure Appl. Opt.*, vol. 10, no. 10, pp. 104022-1–104022-8, 2008.
- [11] K.-P. Yoo and N.-K. Min, "Fabrication of thin-film thermopile microbridge with XeF_2 etching process," *Thin Solid Films*, vol. 516, no. 11, pp. 3586–3589, 2008.
- [12] J. Qu, H. Wu, P. Cheng, Q. Wang, and Q. Sun, "Recent advances in MEMS-based micro heat pipes," *Int. J. Heat Mass Trans.*, vol. 110, pp. 294–313, Jul. 2017.